

Experimental Study of the Effect of Siliconizing Parameters of Thermochemical Treatment of low Carbon Steel

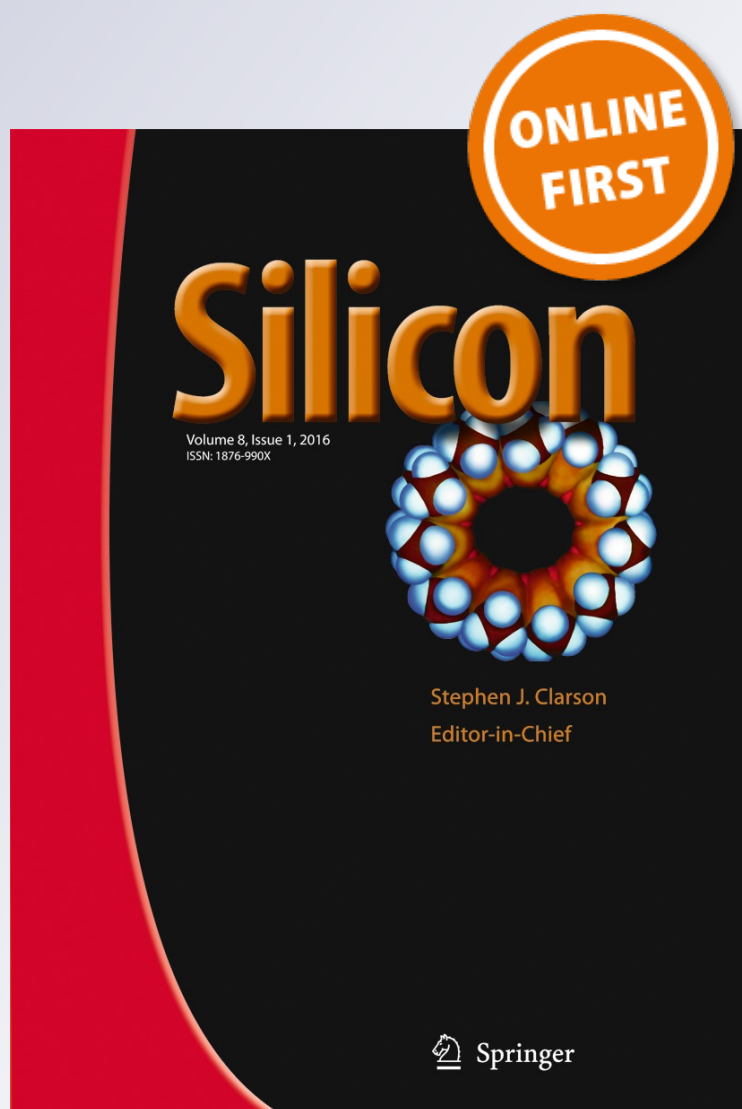
**A. P. I. Popoola, V. S. Aigbodion,
O. S. I. Fayomi & M. Abdulwahab**

Silicon

ISSN 1876-990X

Silicon

DOI 10.1007/s12633-015-9387-3



Your article is protected by copyright and all rights are held exclusively by Springer Science +Business Media Dordrecht. This e-offprint is for personal use only and shall not be self-archived in electronic repositories. If you wish to self-archive your article, please use the accepted manuscript version for posting on your own website. You may further deposit the accepted manuscript version in any repository, provided it is only made publicly available 12 months after official publication or later and provided acknowledgement is given to the original source of publication and a link is inserted to the published article on Springer's website. The link must be accompanied by the following text: "The final publication is available at link.springer.com".

Experimental Study of the Effect of Siliconizing Parameters of Thermochemical Treatment of low Carbon Steel

A. P. I. Popoola¹ · V. S. Aigbodion^{1,2} · O. S. I. Fayomi^{1,3} · M. Abdulwahab^{1,4}

Received: 21 September 2015 / Accepted: 27 November 2015
© Springer Science+Business Media Dordrecht 2016

Abstract In order to use minimum time and save energy during siliconizing surface hardening of low carbon steel it is important to study the siliconizing parameters to obtain optimum conditions. In this work, the experimental design using the Taguchi method is employed to optimize the siliconizing parameters in the pack siliconizing surface hardening process. The siliconizing parameters evaluated are: siliconizing temperature, siliconizing time, silicon potential (ratio of silicon powder to bean pod ash (BPA) nanoparticle) and tempering temperature. The results showed that case depth and hardness values increased exponentially by increasing siliconizing temperature and time. Optimum values of hardness were obtained at a siliconizing temperature of 1000 °C, siliconizing time of 5 hours, silicon potential of 75 wt.% silicon/25 wt.% BPA and tempering temperature of 200 °C. With percentage contribution of: siliconizing temperature (79.86 %), siliconizing time (12.54 %), silicon potential (5.34 %) and tempering temperature (2.26 %).

Silicon powder and bean pod ash nanoparticles can be effective for use as siliconizing materials in the ratio of 75 wt.% silicon/25 wt.% BPA. The activation energy (Q) for research work was determined as 333.89 kJ.mol⁻¹. The growth rate constant (K) ranged from 6.78×10^{-8} to 2.05×10^{-6} m².s⁻¹. The case depth, hardness values and wear rate of siliconized mild steel at these operating conditions can be used for technological and industrial applications such as gears and cams.

Keywords Temperature · Case depth · Time · Hardness · Silicon · Taguchi method and Wear

1 Introduction

Surface Hardening, a process which includes a wide variety of techniques, is used to improve the wear resistance of parts without affecting the more soft, tough interior of the part [1]. This combination of hard surface and resistance to breakage upon impact is useful in parts such as a cam or gear that must have a very hard surface to resist wear, along with a tough interior to resist the impact that occurs during operation [2]. Further, the surface hardening of steel has an advantage over through hardening because less expensive low-carbon and medium-carbon steels can be surface hardened without the problems of distortion and cracking associated with the through hardening of thick sections [3]. There are two distinctly different approaches to the various methods for surface hardening [4]:

- i. Methods that involve an intentional buildup or addition of a new layer
- ii. Methods that involve surface and subsurface modification without any intentional buildup or increase in part dimensions

✉ V. S. Aigbodion
victor.aigbodion@unn.edu.ng

A. P. I. Popoola
popoolaAPI@tut.ac.za

¹ Department of Chemical, Metallurgical and Materials Engineering, Tshwane University of Technology, P.M.B. X680, Pretoria, South Africa

² Department of Metallurgical and Materials Engineering, University of Nigeria, Nsukka, Nigeria

³ Department of Mechanical Engineering, Covenant University, P.M.B 1023, Ota, Ogun State, Nigeria

⁴ Department of Metallurgical and Materials Engineering, Ahmadu Bello University, Zaria, Nigeria

Table 1 Chemical Composition of the mild steel

Element	C	Si	Mn	P	S	Cr	Mo	Ni	Sn	Cu	V
Percent	0.13	0.15	0.47	0.043	0.006	0.01	0.01	0.01	0.001	0.03	0.002

The first group of surface hardening methods includes the use of thin films, coatings, or weld overlays (hardfacings) [5]. Films, coatings, and overlays generally become less cost effective as production quantities increase, especially when the entire surface of workpieces must be hardened [6]. The fatigue performance of films, coatings, and overlays may also be a limiting factor, depending on the bond strength between the substrate and the added layer [7]. Fusion-welded overlays have strong bonds, but the primary surface-hardened steels used in wear applications with fatigue loads include heavy casehardened steels and flame- or induction-hardened steels. Nonetheless, coatings and overlays can be effective in some applications [8]. With tool steels, for example, TiN and Al₂O₃ coatings are effective not only because of their hardness but also because their chemical inertness reduces crater wear and the welding of chips to the tool [9].

Surface hardening focuses exclusively on the second group of methods, which is further divided into diffusion methods and selective hardening methods [10]. Diffusion methods modify the chemical composition of the surface with hardening species such as carbon, nitrogen, silicon or boron. Diffusion methods allow effective hardening of the entire surface of a part and are generally used when a large number of parts are to be surface hardened. In contrast, selective surface hardening methods allow localized hardening [11]. Selective hardening generally involves transformation hardening (from heating and quenching), but some selective hardening methods (selective nitriding, ion implantation and ion beam mixing) are based solely on compositional modification [12].

Siliconizing involves the diffusion of silicon into metal surfaces for the enhancement of hardness and wear resistance. Siliconizing techniques include metallizing, chemical vapor deposition, and pack cementation [13]. There are a lot of bean pod waste materials, this waste constitute a nuisance to the environment not only in Africa but the in world at large. The ability to convert these wastes into useful engineering materials e.g as filler materials in the siliconizing process sharpens the focus of this present research work. From the available literature no investigation has been conducted on the application of the bean pod ash nanoparticles as filler materials in the siliconizing process. A relationship between the mechanical properties of the siliconized mild steel and the siliconizing process parameters (siliconizing temperature and time, ratio of silicon to bean pod ash (BPA) nanoparticles, tempering temperature) will provide better understanding of the mechanical properties. Based on

the above-mentioned situation, this work intends to study the empirical model for estimating mechanical properties of siliconizing of mild steel using silicon powder and BPA nanoparticles.

2 Materials and Method

2.1 Materials

The materials used for the work included mild steel rods of 16 mm diameter. The chemical composition of mild steel was determined by metal spectrometry and the result is shown in Table 1. BPA nanoparticles of 55 nm were used in this research, details of the production of the nanoparticles has been described elsewhere by us [14]. The SEM morphology is shown in Fig. 1. From the SEM it is observed that the BPA nanoparticles are roundish with some angular in shape and a small amount of particles longitudinal in shape. Equipment used in this research are: Drying oven, muffle type furnace, Pyrometer, Rockwell hardness Testing Machine Model MHT-1 No: 8331 made by Matsuzawa Seiki Co. Ltd., of Japan, Pin-on-disc machine (make: SD scientific industries), Grinding and Polishing machine, Scanning Electron Microscopy (SEM)/Energy dispersive system (EDS), Optical Metallurgical Microscope, X-ray diffractometer(XRD).

2.2 Method

2.2.1 Design of Experiment Using Taguchi Method

In this research, the design of experiment by Taguchi was used. The operating parameters used in this study are shown

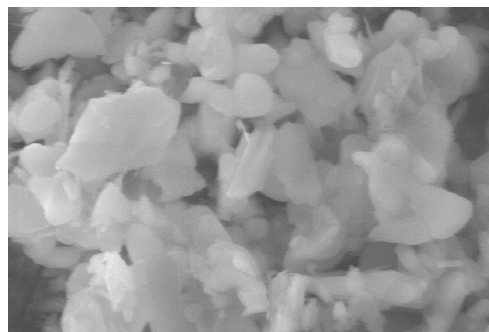
**Fig. 1** SEM microstructure of BPA nanoparticles

Table 2 Operating parameters

Serial no	Control variable	Notations	Value with range
1	Siliconizing Temperatures (°C)	A	800-1000
2	Siliconizing Time (hours)	B	1-5
3	Ratio of pure silicon to developed silicon (wt.%)	C	85:15-65:35
4	Tempering Temperatures (°C)	D	200-300

in Table 2, while Table 3 gives the number of levels and process parameters. The (L9) orthogonal array with four columns and nine rows was employed (see Table 4). The four process variables namely, siliconizing temperature, siliconizing time, tempering temperature and siliconizing materials, which affect the hardness, case depth and wear rate were selected for the Taguchi design. A L9 (3⁴) orthogonal array design was adopted for experimentation. The 9 experiments were conducted by varying all the parameters and a study of the influence of these parameters (between low, medium and high) on surface hardness was used for the optimization of the process.

A parameter design study involves control and noise factors. The measure of interaction between these factors with regard to robustness is the signal-to-noise (S/N) ratio. The signal-to-noise ratio was used to measure the sensitivity of the quality characteristic being investigated in a controlled manner. In the Taguchi method, the term ‘signal’ represents the desirable effect (mean) for the output characteristic and the term ‘noise’ represents the undesirable effect (signal disturbance, S.D) for the output characteristic which influences the outcome due to external factors namely noise factors. The S/N ratio can be defined as:

$$S/N \text{ ratio, } \eta = -10 \log (\text{MSD}) \tag{1}$$

Where MSD is the mean-square deviation for the output characteristic. The aim of any experiment is always to determine the highest possible S/N ratio for the result. A high value of S/N implies that the signal is much higher than the random effects of the noise factors or minimum variance. There are three categories of quality characteristics, i.e. the lower-the-better, the higher-the-better, and the

nominal-the-better. To obtain optimal response performance, the higher-the-better quality characteristic for hardness must be taken. The mean-square deviation (MSD) for the higher-the-better quality characteristic of the hardness values was expressed as:

$$\text{MSD} = (1/n(1/y_{12} + 1/y_{22} \dots 1/y_{n2})) \tag{2}$$

Where, n = number of repetitions or observations y_i = the observed data. ANOVA analysis of the hardness values was carried out to determine the influence of main variables on surface hardness and also to determine the percentage contributions of each variable.

$$\text{Correction factor, C.F} = [\sum y_i^2 / \text{Number of Experiments}] \tag{3}$$

$$\text{Total sum of squares, SST} = \sum y_i^2 - \text{C.F} \tag{4}$$

$$\text{Variable of SS} = [\sum y_{12}^2/3 + \sum y_{22}^2/3 + \sum y_{32}^2/3] - \text{C.F} \tag{5}$$

$$\text{Percentage contribution of each variable} = (\text{SSA}/\text{SST}) * 100 \tag{6}$$

2.2.2 Siliconizing of Mild Steel Samples

The different test specimen samples made up of mild steel for mechanical and wear properties testing were subjected to

Table 3 Number of level and process parameters

Control variables	Level			Observed values
	1	2	3	
	Low	Middle	High	
Siliconizing temperatures (°C)	800	900	1000	Hardness values (HRC)
Siliconizing time (hours)	1	3	5	
Ratio of pure silicon to BPA (wt.%)	85:15	75:25	65:35	
Tempering temperatures (°C)	200	250	300	

Table 4 Design layout of experiments using the orthogonal array

Control Variables	Siliconizing Temperatures (°C)	Siliconizing time (hours)	Ratio of pure silicon to BPA (wt.%)	Tempering Temperatures (°C)
EXP No				
S1	1	1	1	1
S2	1	2	2	2
S3	1	3	3	3
S4	2	1	2	3
S5	2	2	3	1
S6	2	3	1	2
S7	3	1	3	2
S8	3	2	1	3
S9	3	3	2	1

siliconizing treatment. In this process the mild steel samples containing silicon powder and BPA nanoparticle powder were placed in a graphite crucible and fully covered from all sides and the top of the container was covered with a steel plate. The container was then placed into the muffle furnace and maintained at the different required siliconizing temperatures and times as shown in Table 4. By this way the mild steel samples are siliconized and then they were quenched in water. The siliconized steel samples were then tempered for 2 hours.

2.2.3 Tempering of Siliconized Mild Steel Samples

After the siliconizing process, the steel is often harder than needed and is too brittle for most practical uses. Also, severe internal stresses are set up during the rapid cooling from the hardening temperature. To relieve the internal stresses and reduce brittleness, the siliconized steel should be tempered. Tempering of the siliconized steel samples was done in a muffle furnace at the temperatures and times shown in Table 4 and cooling was done in still air. The siliconized

and tempered mild steel specimens were then subjected to various mechanical and wear tests.

2.2.4 Hardness Testing and Effective Case Depth Determination

Steel discs of 15 mm thick were cut from the central region of each of the siliconized specimens. They were prepared and polished for hardness measurement on a Rockwell hardness indenter. Hardness measurements on all the specimens were carried out on a Rockwell hardness Testing Machine Model MHT-1 No: 8331 made by Matsuzawa Seiki Co.Ltd., of Japan. From the hardness values obtained for each specimen, hardness profiles were plotted and effective case depths at various times were extracted.

2.2.5 Abrasive Wear Test

The materials considered for this experiment was siliconized and tempered mild steel samples under different levels in Table 4. The test was conducted on a Pin-on-disc

Table 5 Results of the design layout of experiments using the orthogonal array

Control variables	Hardness values (HRC)	Average case depth (mm)	Wear rate (g/m) × 10 ⁻⁶
EXP No			
Control	35.67	nil	5.50
S1	42.89	1.35	4.02
S2	43.89	1.50	3.79
S3	46.78	1.58	3.65
S4	47.12	1.60	3.01
S5	48.45	1.79	2.85
S6	47.91	1.64	3.00
S7	50.79	1.97	2.65
S8	51.04	2.01	2.52
S9	56.68	2.40	2.44

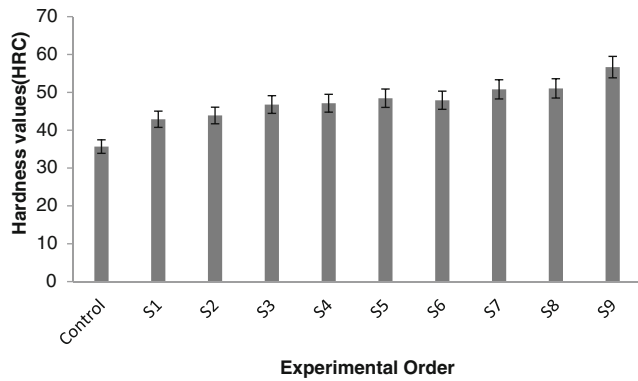


Fig. 2 Variation of Hardness values with the experimental order

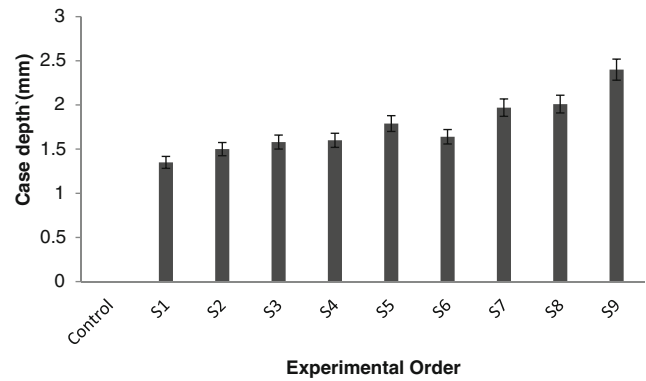


Fig. 4 Variation of case depth with the experimental order

machine (make: SD scientific industries). In this experiment the test was conducted with a of speed of 2.5 m/s, sliding distance of 2000 m and load of 50 N. The formula used to convert the weight loss into wear rate is:

$$\text{Wear rate} = \frac{\Delta W}{S} \quad (7)$$

Where ΔW is the weight difference of the sample before and after the test in g, S is total sliding distance in m.

2.2.6 Microstructure and Phase Analysis

X-ray diffraction (XRD) analyses were carried out using a X'Pert Pro model diffractometer to identify the phases present on the resulting siliconized layer. A Cu $K\alpha$ radiation source on the X'Pert Pro diffractometer set at 40 kV and 20 mA was used to scan in a range between 10° and 80° two theta (2θ) with a step size of 0.02° . The microstructure siliconized sample was studied using a JOEL JSM 5900LV Scanning Electron Microscope equipped with an Oxford INCA™ Energy Dispersive Spectroscopy (EDS) system. The SEM was operated at an accelerating voltage of 5 to 20 kV.

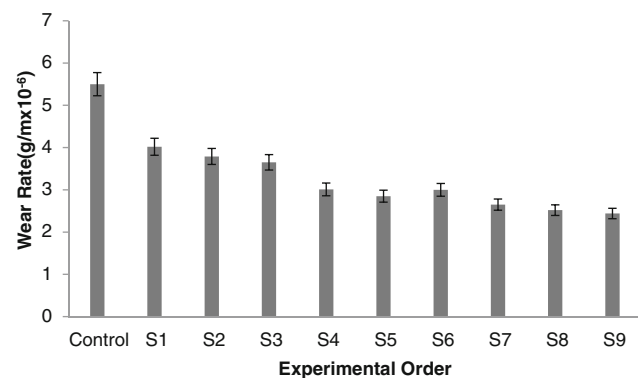


Fig. 3 Variation of wear rate with the experimental order

3 Results and Discussion

3.1 Effect of Siliconizing Parameter

The hardness values of the unsiliconized sample is 35.67 HRC and after siliconizing the hardness values rise to 42.89 HRC – 56.68 HRC showing that siliconizing of the sample resulted in an increase in hardness under the different conditions. The wear rate of the unsiliconized sample was 5.50×10^{-6} g/m and that of siliconized samples ranges from 4.02 to 2.44×10^{-6} g/m, the siliconized samples case depth ranges from 1.35 to 2.40 mm respectively (see Table 5 and Figs. 2, 3 and 4).

The effects of temperature on hardness, wear rate and case depth of siliconized samples are shown in Table 5 and Figs. 2–4. The results show that the siliconizing process greatly improves the hardness, wear rate and case depth of the samples. The results explain that the hardness, wear rate and case depth varied directly with the increase in siliconizing temperature. With the increase in the siliconizing temperature, the hardness, wear rate and case depth increase linearly with siliconizing temperature of 800, 900 and 100 °C. The highest hardness values of the siliconized sample occurred at 100 °C (level 3) and the lowest at 80 °C (level 1).

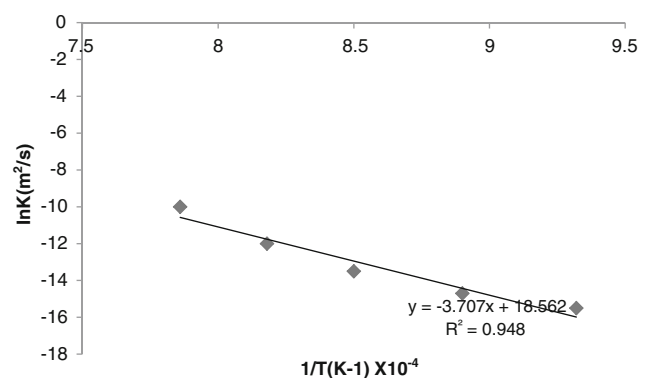
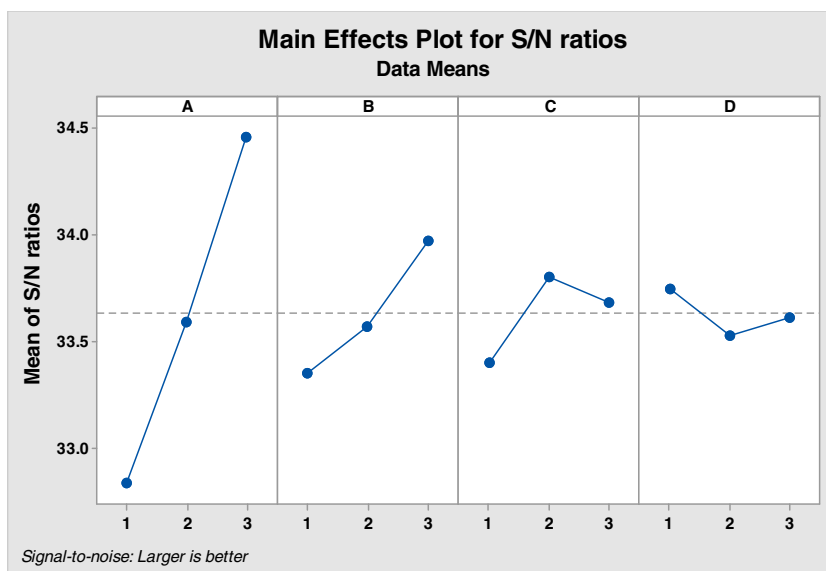


Fig. 5 Growth rate constant vs. temperature of siliconized mild steel

Fig. 6 Variation of mean of S/N ratios with the experimental levels



This may be attributed to an increase in the percentage of silicon released into the steel sample as the temperature increases.

The effect of siliconizing time shows similar results as that of siliconizing temperature. As the siliconizing time increases from 1.0 hours (level 1) to 5.0 hours (level 3) the hardness values, wear rate and case depth of the siliconized mild steel quenched also improved (see Table 5 and Figs. 2–4). Due to the large difference in silicon potential between the rich silicon atmosphere and the surface of the alloy there is an increased rate of absorption of diffusing silicon atoms into the alloy as the siliconizing time rises from 1.0 to 5.0 hours. The decrease in hardness values and case depth at low siliconizing time is a result of the low rate of diffusion of silicon. This shows that the lattices of the austenite phase are almost saturated with silicon with the increase in temperature and silconizing time. Also as siliconizing temperatures and time increase the lattices of the austenite phase are saturated and result in the formation of hard phases of Fe₂Si, FeSi in the steel sample. This observation agrees with previous studies [4, 9].

Table 5 and Figs. 1–3 show the average case depth, hardness values and wear rate obtained with various siliconizing compositions. It can be observed that at 75 wt.% silicon/25 wt.% BPA at level 2 had the highest average case depth of 2.40 mm, 56.68 HRC hardness values and lower wear rate of 2.44×10^{-6} g/m. The increase in the average case depth, hardness values and low wear rate can be ascribed to the ability of BPA to supply filler materials during the siliconizing process. This is attributed to the fact that BPA contains SiO₂. Other researchers have observed the same [14]. For the siliconizing composition 65 wt.% silicon/35 wt.% BPA at level 3 the hardness value and case depth decrease may be attributed to the decrease in the weight percentage of the silicon which acts as the silicon potential. It can be concluded that optimized conditions can be obtained at 75 wt.% silicon/25 wt.% BPA at level 2.

Table 5 and Figs. 1–3 show the average case depth and hardness values decreasing as the tempering temperatures increased from 200 °C (level 1) to 400 °C (level 3). The samples tempered at 200 °C (level 1) had the highest

Table 6 The signal to noise ratio

S/N	T ₁	T ₂	T ₃	S/N ratio
1	41.83	41.94	42.89	32.4415
2	44.94	43.84	43.90	32.8480
3	45.79	44.82	45.77	33.2160
4	47.10	47.19	47.13	33.4678
5	49.44	48.41	48.50	48.50
6	47.94	47.87	48.91	33.6079
7	50.87	51.89	50.92	34.1332

T₁, T₂ and T₃ represent values for the three repetitions of each trial.

Table 7 ANOVA for Model

Source	Sum of squares	Hardness values			P _{value}	% Contribution	Remarks
		DF	Mean square	F _{value}			
Model	142.64	4	35.66	13.16	0.0164		Significant
A	123.27	2	61.64	21.02	0.0076	79.86	Significant
B	9.36	2	9.68	3.30	0.1424	12.54	Not significant
C	7.43	2	7.43	42.07	0.174	5.34	Not significant
D	0.67	2	0.67	4.29	0.1300	2.26	Not significant
Residual	12.73	4	2.93				
CorTotal	154.37	8					

average case depth of 2.40 mm, 56.68 HRC hardness values and lower wear rate of 2.44×10^{-6} g/m. Through carefully controlled tempering treatment, the quenching stresses can be relieved and some of the silicon can precipitate from the supersaturated solid solution to a finely dispersed silicon phase. The properties of the tempered steel are primarily determined by the size, shape, composition and distribution of the silicon phase that forms with a relatively minor contribution from the solid solution hardening of the ferrite.

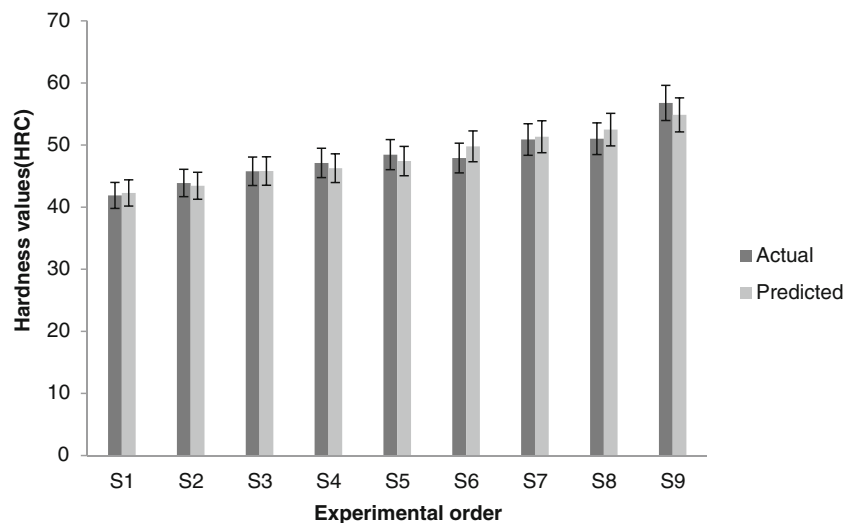
By using the Arrhenius equation (see Eq. 8) and by taking the relationship between the diffusion coefficients (growth rate constant), K (m^2s^{-1}), activation energy(Q) ($J.mol^{-1}$) and the process temperature in Kelvins (T) the activation energy of the siliconizing process can be obtained.

$$K = K_0 e^{-\frac{Q}{RT}} \tag{8}$$

Where K_0 is the frequency factor and R is the gas constant. Taking the natural logarithm it can be derived as follows:

$$\ln K = \ln K_0 - \frac{Q}{RT} \tag{9}$$

Fig. 7 Validation of mathematical model



The plot of $\ln K$ versus reciprocal treatment temperature is linear as shown in Fig. 5. The activation energy was calculated from the slope of Fig. 5. The value of K rises with treatment temperature. Activation energy (Q) for research work was determined as $333.89 \text{ kJ.mol}^{-1}$. The growth rate constant (K) ranged from 6.78×10^{-8} to $2.05 \times 10^{-6} \text{ m}^2.s^{-1}$. The result obtained for the activation energy in this work is in agreement with that of Yang et al [8] who reported that the activation energy of silicon in the silicide layer is between 643 and 242 kJmol^{-1} at siliconizing temperatures of 900 to 1000 °C. The regression coefficient in Fig. 4 is 0.948 which is close to unity(1).

3.2 Effect of Signal to Noise Ratio and Analysis of Variance (ANOVA) of the Hardness Values

Figure 6 and Table 6 show the S/N ratio graphs where the horizontal line is the value of the total mean of the S/N ratio. Basically the larger the S/N ratio the better are the quality characteristics for the process. For the S/N ratio analysis from the graphs the levels of parameters to be set for getting optimum values of hardness are siliconizing temperature

(A) of 1000 °C (level 3), siliconizing time (B) 5.5 hours (level 3), Silicon potential (C) of 75 wt.% silicon/25 wt.% BPA (level 2) and tempering temperature (D) of 200 °C (level 1). The ANOVA analysis is shown in Table 7. The Model F-value of 13.16 implies the model is significant. There is only a 1.54 % chance that a “Model F-Value” this large could occur due to noise. Values of “Prob >F” less than 0.0500 indicate the model terms are significant. In this case A (siliconizing temperature) is significant in model terms. The percentage contributions of siliconizing time B is (12.54 %), silicon potential C (5.34 %) and siliconizing temperature (79.86 %). The confirmation of the experiment showed that the observations are within a 95 % confidence level. The error in the experimental analysis is very low, and hence Taguchi’s techniques were successfully applied to determine the optimum process parameters for siliconizing the steel in order to achieve quality components. The “Pred R-Squared” of 0.8153 is close to the “Adj R-Squared” of 0.8480 with Std. Dev. 1.71 and mean of 48.19.

The regression equation for the response characteristics as a function of two input parameters of the material considered in this experiment is given below. In this case the regression equation is formulated in terms of the

siliconizing parameters. The final equation in terms of coded factors using design expert 6.0 software is:

$$\text{Hardness values} = +48.19 - 4.44 * A[1] - 0.38 * A[2] - 1.66 * B[1] - 0.42 * B[2] \quad (10)$$

In order to validate the regression equations, experimental data were compared with data obtained by putting the different experimental conditions in the regression equation. The results are given in Fig. 7. The result in Fig. 7 shows that the experimental data and data obtained by the regression equation are in close correlation. The percentage of error was calculated using Eq. 11 for the validation of the regression model

$$\% \text{ of error} = (\text{Actual value} - \text{Predicted value}) / \text{Actual value} * 100 \% \quad (11)$$

From Fig. 6 the average absolute error for the hardness values is 1.75 % which means that a better accuracy was obtained using the developed regression model.

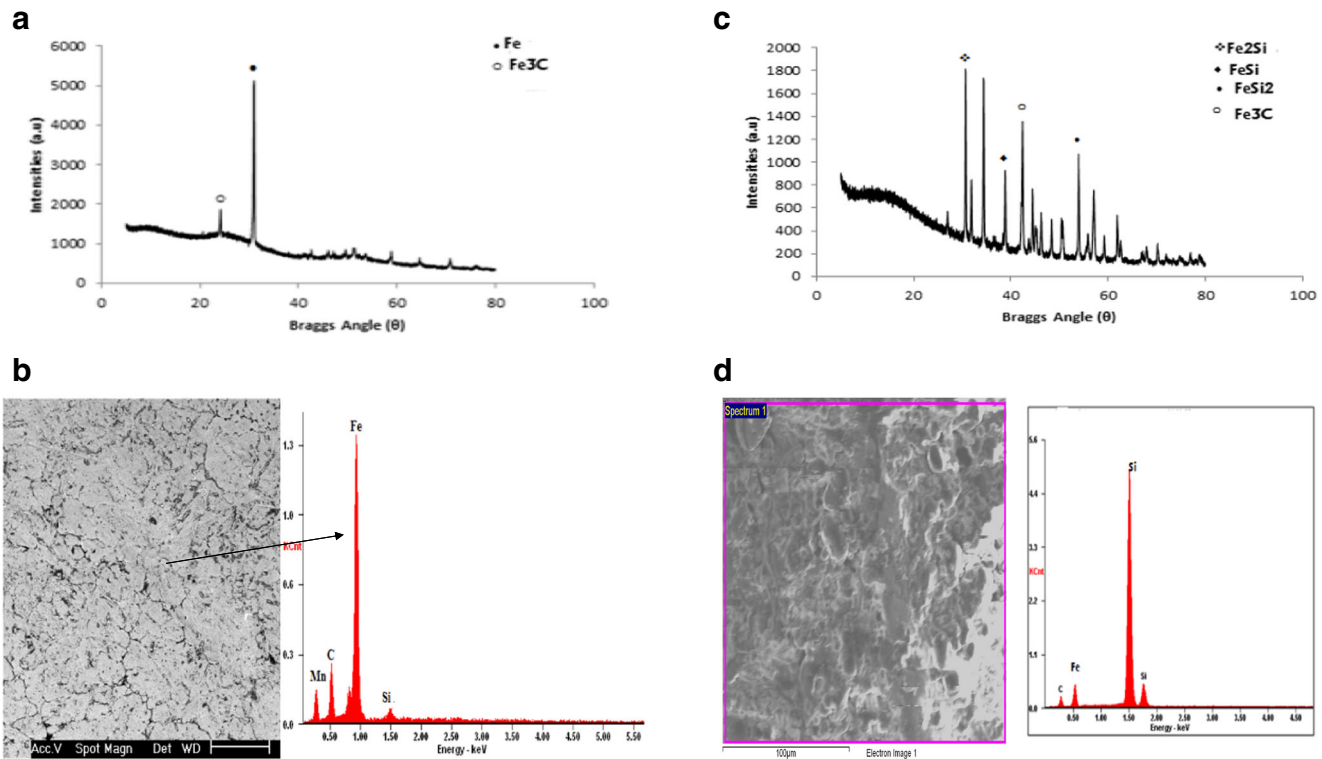


Fig. 8 a XRD spectrum of the substrate (Mild Steel). b SEM/EDS morphology of the mild steel. c XRD spectrum of the siliconized mild steel at optimum condition. d SEM/EDS of the siliconized mild steel at optimum condition

3.3 XRD and Microstructure of the Siliconized Samples

The XRD spectrum of the mild steel used for the research is shown in Fig. 8a, From Fig. 8a, it is clear that a high peak of α -Fe (ferrite phase) occurred at 34.5° and with a low peak of Fe_3C (cementite) at 27.1° . The higher α -Fe peak than the peak of Fe_3C in the XRD spectrum confirmed the composition in Table 1 that the substrate is mild steel. Figure 8b shows the SEM/EDS analysis of the mild steel used for the experiment. The SEM morphology clearly shows a pearlite (dark) phase in the ferrite matrix (white). The ferrite phase region is larger in the SEM than the pearlite phase. The energy dispersive spectrometry analysis revealed major peaks of Fe and C with some minor peaks of Mn and Si. The high peaks of Fe and C confirmed that the steel used in this work is mild steel.

Figure 8c shows the XRD spectrum of the siliconized hardened surface of mild steel at optimum conditions. From Fig. 8c it can be observed that there is a great difference to the XRD spectrum in Fig. 8a. In Fig. 8c one can see the hard silicide layer of phases formed on the siliconized steel which consists of Fe_2Si , FeSi and FeSi_2 phases. It is clear from the SEM that the surface of the siliconized steel has a great morphological change in the microstructure of the substrate after siliconizing (compare Fig. 8b with Fig. 8d). EDS analysis in Fig. 8d shows that silicon atoms in the siliconized layer are more concentrated in the outer layer of the siliconized layer than in the inner part. The silicon content close to the outer surface of the coating layer is higher than the inner part of the coating layer as shown in EDS analysis Fig. 8b. EDS analysis shows that the iron concentration in the silicide layer is lower than the inner part. There is evidence of high silicon peaks in Fig. 7d which are responsible for the formation of a hard silicide layer of Fe_2Si , FeSi and FeSi_2 phases. These silicide phases forming at the surface are one of the principal mechanisms for the high hardness values and wear resistance of the siliconized samples.

4 Conclusions

This study has presented an investigation on the optimization and the effect of siliconizing parameters on the hardness, case depth and wear rate of mild steel of samples. From the results and discussions above the following conclusions can be made:

1. Case depth and hardness values increased exponentially by increasing siliconizing temperature and time.
2. The samples having greater case depth and surface hardness are more wear resistant than those with low case depth and low surface hardness.
3. Optimum values of hardness were obtained at a siliconizing temperature of 1000°C , siliconizing time 5 hours, silicon potential of 75 wt.% silicon/25 wt.% BPA and tempering temperature of 200°C .
4. The level of importance of the siliconizing parameters on the hardness is determined by using ANOVA. Based on the ANOVA method, the highly effective parameters on hardness found that the siliconizing temperature (78.86 %) has the higher significant effect on the hardness surface than siliconizing time (13.54 %), silicon potential (5.44 %) and tempering temperature (2.26 %).
5. Silicon powder and bean pod ash nanoparticles can be effectively used as siliconizing materials in the ratio of 75 wt.% silicon powder: 25 wt.% BPA.
6. The activation energy (Q) was determined as $333.89 \text{ kJ.mol}^{-1}$. The growth rate constant (K) ranged from 6.78×10^{-8} to $2.05 \times 10^{-6} \text{ m}^2.\text{s}^{-1}$.

Acknowledgments This material is based upon work supported financially by the National Research Foundation. Tshwane University of Technology, Pretoria is appreciated for support which aided the accomplishment of this work.

References

1. Ihom AP, Yaro SA, Aigbodion VS (2005) The effect of carburisation on the corrosion resistance of mild steel in four different media. *J Corros Sci Technol* 3:18–21
2. Ihom AP, Nyior GB, Alabi OO, Segun S, Nor II, Ogbodo JN (2012) The potentials of waste organic materials for surface hardness improvement of mild steel. *Int J Sci Eng Res* 3(11):1–20
3. Wang Kf, Chandrasekar S, Yang Hty (1997) Experimental and computational study of the quenching of carbon steel. *Intl JI Manufact Sci Eng* 119(3):257–65
4. Palaniradja K, Alagumurthi N, Soundararajan V (2010) Hardness and case depth analysis through optimization techniques in surface hardening processes. *Open Mater Sci J* 4:38–63
5. Liu CC, Xu X, Liu ZA (2003) FEM modeling of quenching and tempering and its application in industrial engineering. *Finite Elem Anal Des* 39(11):1053–70
6. Pierre D, Peronnet M, Bosselet F, Viala JC, Bouix J (2002) Chemical interaction between mild steel and liquid Mg-Si alloys. *Mater Sci Eng B* 94:186–195
7. Gasa P, D'heurleb FM (1993) Formation of silicide thin films by solid state reaction. *Appl Surf Sci* 73:153–161
8. Yang HL, Cui CW, Li YG, Tang GZ, Zhang YZ (2011) Growth kinetics and microstructure of siliconized layer by molten salt electrodepositi. *Adv Mater Res* 214:434–438

9. Perez-Mariano J, Elvira J, Plana F, Colominas C (2006) Siliconization and nitridation of steels in a fluidized bed reactor. *Surf Coat Technol* 200:5606–5610
10. Grünling HW, Bauer R (1982) The role of silicon in corrosion-resistant high temperature coatings. *Thin Solid Film* 95:3–20
11. Stott FH, Wei FI (1989) Comparison of the effects of small additions of silicon or aluminum on the oxidation of iron-chromium alloys. *Oxid Met* 31:369–39
12. Basu SN, Yurek GY (1991) Effect of alloy grain size and silicon content on the oxidation of austenitic Fe-Cr-Ni-Mn-Si alloys in pure O₂. *Oxid Met* 36:281–315
13. Hsu HW, Tsai WT (2000) High temperature corrosion behavior of siliconized 310 stainless steel. *Mater Chem Phys* 64:147–155
14. Atuanya CU, Aigbodion VS (2014) Evaluation of Al-Cu-Mg alloy/bean pod ash nanoparticles synthesis by double layer feeding–stir casting method. *J Alloys Compd* 601:251–259